

Equivalent static wind loads for stability design of large span roof structures

Ming Gu^{*1} and Youqin Huang^{2a}

¹State Key Laboratory of Disaster Reduction in Civil Engineering, Tongji University, 1239 Siping Rd., Yangpu District, Shanghai, P.R. China

²Engineering Technology Research and Development Center for Structural safety and Health Monitoring in Guangdong Province, Guangzhou University, 230 West Wai'huan RD., Higher Education Mega Center, Guangzhou, P.R. China

(Received July 20, 2014, Revised November 20, 2014, Accepted December 6, 2014)

Abstract. Wind effects on roofs are usually considered by equivalent static wind loads based on the equivalence of displacement or internal force for structural design. However, for large-span spatial structures that are prone to dynamic instability under strong winds, such equivalent static wind loads may be inapplicable. The dynamic stability of spatial structures under unsteady wind forces is therefore studied in this paper. A new concept and its corresponding method for dynamic instability-aimed equivalent static wind loads are proposed for structural engineers. The method is applied in the dynamic stability design of an actual double-layer cylindrical reticulated shell under wind actions. An experimental–numerical method is adopted to study the dynamic stability of the shell and the dynamic instability originating from critical wind velocity. The dynamic instability-aimed equivalent static wind loads of the shell are obtained.

Keywords: spatial structures; structural instability; Budiansky–Roth criterion; dynamic instability-aimed equivalent static wind loads; application

1. Introduction

Numerous spatial structures have been constructed all over the world given their beautiful appearance and good spanning capability. Over the years, however, many structural failures have occurred under strong winds (Shanmugasundaram *et al.* 2000, Duthinh 2008). The loss of the stable equilibrium state can be one of the reasons for structural collapse under strong wind actions; such occurrences in China have been documented (Huang and Gu 2011). These incidents have highlighted the necessity of analyzing the instability in the structural design of spatial structures (Ministry of Housing and Urban-Rural Development of the People's Republic of China 2003). To avert structural failures, more precise methods for dynamic stability design should be proposed and adopted in structurally designing spatial structures that are prone to wind-induced dynamic instability.

The characteristics of structural dynamic instability in spatial structures are complicated, and

*Corresponding author, Professor, E-mail: minggu@tongji.edu.cn

^a Ph.D., E-mail: yqhuang@gzhu.edu.cn

significant studies have been conducted by many researchers (Hsu 1967, Simitsev 1990, Ishikawa and Kato 1993, Sofiyev 2004). The wind-induced instability of spatial structures is generally investigated through wind tunnel tests. Miyake *et al.* (1992) observed the stability of a suspended roof model in a wind tunnel test. Nakamura *et al.* (1994) found that the displacement responses of a large-span roof aeroelastic model grew nearly exponentially with wind speed in a wind tunnel test. Meanwhile, some researchers studied the instability of spatial structures due to wind action using numerical methods. He (2002) derived a formula for galloping critical wind speed as a function of the shape coefficient by considering the initial attack angle and lateral aerodynamic forces. Yang and Liu (2005) studied the unstable state originating from the critical wind velocity of membrane structures by combining non-moment theory for thin shallow shells and potential flow theory for fluids. Cao *et al.* (2010) analyzed the stability, deformation, and stress distribution of a flexible container roof under strong winds using the arbitrary Lagrangian–Eulerian approach. When Li and Tamura (2005) conducted the nonlinear dynamic analysis of a single-layer spherical reticulated shell subjected to wind loads, they suggested that the dynamic instability of spatial structures can be investigated by examining their tangent stiffness matrixes and computational divergence. In this paper, the instability of roof structures under unsteady wind forces is also investigated by the response divergence according to the classic Budiansky–Roth criterion (Budiansky and Roth 1962).

The equivalent static wind load (ESWL) is a concept that bridges wind engineering research and structural engineering applications. It plays an important role in the wind resistance design of structures. After Davenport (1961) shed light on the concept of ESWL, the dynamic wind effects on structures have since then been computed using the ESWL for structural design. Davenport (1967) proposed the gust loading factor (GLF) in considering the magnification of structural response to turbulent wind loads. In his study, the ESWL for structural design was equal to the mean wind loads multiplied by the GLF. Kasperski (1992) put forward the load–response–correlation (LRC) method, which is a quasi-static method for calculating the ESWL on rigid structures. The two achievements mentioned above pose considerable significance to the collaboration between wind engineering researchers and structural engineers. Zhou *et al.* (1999) built the form of ESWL on high-rise buildings by dividing it into the mean, background, and resonant components based on the work by Davenport (1961, 1995). The background component can be computed using the LRC method and the resonant component can be calculated using structural inertia forces caused by vibration. Fu *et al.* (2008) presented a new definition of the ESWL on long-span roof structures expressed in terms of the mean and dynamic components and based on the LRC method. Such ESWL eliminates the shortcomings of the zero mean response of the GLF method, considers modal response correlations and does not require the calculation of the load–response correlation. Bartoli and Ricciardelli (2010) investigated the characteristics of pressure fluctuations in the ESWLs on structures. For the high-rise building with the eccentricity of the mass center with respect to rigidity or geometry center more than 10%, Liang *et al.* (2014) pointed out that the along-wind, cross-wind and torsional responses are coupled, and then constructed the three-dimensional static wind loads based on the equivalence of internal forces. Ke *et al.* (2014) studied the wind-induced response and equivalent static wind loads of large wind turbines by the modified consistent coupling method.

Considering the characteristics of multiple targets of equivalence in the ESWLs of large span roofs, Katsumura *et al.* (2007) presented the universal ESWL to achieve the equivalence of all responses in the structure by choosing the intrinsic modes of fluctuating wind load as the basic load vectors. Chen *et al.* (2012) further selected the initial forces of structural dominating vibration

modes as the basic vectors, enhancing the physical significance of the ESWL for multiple targets. Zhou *et al.* (2012) adopted the response grouping approach to construct such ESWLs.

Despite these developments, however, all of these ESWL methods are essentially based on the equivalence of displacements or internal forces. When they are adopted for the stability analysis of structures, the correspondence between structural instability under such ESWLs and actual dynamic instability that originates from critical wind velocity is difficult to accomplish.

To enable structural engineers to conduct the stability analysis of spatial structures under unsteady wind loads by a static load method, it is necessary to study the ESWLs based on the equivalence of dynamic stability, that is, dynamic instability-aimed ESWLs. In the present study, a new concept of dynamic instability-aimed ESWLs and its corresponding method are proposed. These are applied in the dynamic stability design of a double-layer cylindrical reticulated shell under wind actions. An experimental–numerical method is employed to investigate the dynamic stability of the shell under unsteady wind forces, whose values have been obtained from a wind tunnel test. The state of the dynamic instability of the structural system is determined by the Budiansky–Roth criterion (B–R criterion). Finally, some related aspects of the new concept are discussed in detail, and suggestions for the dynamic stability design of spatial structures under wind loads are provided.

2. Theory and method

The application of the B–R criterion is first introduced, and then the concept of dynamic instability-aimed ESWLs is presented. Finally, the method for applying this concept in the dynamic stability design of spatial structures is explained.

2.1 Application of the Budiansky–Roth criterion

Budiansky and Roth (1962) put forward the B–R criterion to determine the critical load for the dynamic instability of a clamped shallow spherical shell under transient pressure loads. In the B–R criterion, the nonlinear dynamic analysis of structural systems under dynamic loads should be conducted to obtain the variation curve of the largest structural response with the increasing load. When a very deep rise occurs in a small change of the load, this load can be denoted as the critical load for dynamic instability. This criterion is appropriate for both conservative and non-conservative structural systems; thus, it is widely used in studying the dynamic stability of complex structural systems under arbitrary dynamic loads (Song and Jones 1983, Toi and Isobe 1996).

In the present study, the B–R criterion is also adopted to determine the state of dynamic instability of spatial structures under dynamic wind actions, in which the maximum displacement response of the structure is obtained by dynamic response analysis that is based on a proportional loading strategy. Wind load incremental factor f is defined to increase the unsteady wind forces on the structure

$$F_{ij} = f \cdot F_{0ij} \quad (1)$$

where F_{ij} represents the actual wind forces acting on the structure; F_{0ij} denotes the wind forces that corresponds to the design wind velocity of the structure. Therefore, f denotes the actual wind

forces divided by the design wind forces on the structure, and \sqrt{f} denotes the actual wind velocity divided by the design wind velocity of the structure.

The maximum displacement response of a structure under the action of wind forces F_{ij} corresponding to specified f is defined as

$$w_{\max}(f, T) = \max_{0 \leq t \leq T} [w(f, t)] \quad (2)$$

where w_{\max} is the maximum displacement response of the structure; f is the wind load incremental factor; T denotes the length of wind duration, that is, record length T_{total} at full scale; t represents the acting moment of unsteady wind forces; and w is the displacement response of every node of the structure at t under specified f . Therefore, w_{\max} denotes the maximum value of the displacement responses of all the nodes of the structure during entire duration T of wind actions that correspond to load incremental factor f .

2.2 Concept of dynamic instability-aimed ESWLs

The concept of dynamic instability-aimed ESWLs is presented through the GLF method (Davenport 1967). “Dynamic instability factor” φ_D is defined to express the influence of the dynamic actions of wind loads on structural stability. Thus, dynamic instability-aimed ESWLs $\hat{p}(x, y, z)$ on the structure can be expressed as

$$\hat{p}(x, y, z) = \varphi_D \cdot \bar{p}(x, y, z) \quad (3)$$

where $\bar{p}(x, y, z)$ is the mean wind load corresponding to the design wind velocity of the structure, and dynamic instability factor φ_D is determined by

$$\varphi_D = \frac{f_S}{f_D} \quad (4)$$

where f_S and f_D are the critical wind load incremental factors, as determined by the nonlinear static and dynamic stability analyses of the structural system, respectively.

f_S is determined by the static stability analysis under proportionally increasing load of $f \cdot \bar{p}(x, y, z)$. f_D is determined by the B–R criterion described in Section 2.1.

When the ESWLs $\hat{p}(x, y, z)$ are used for structural stability design, another wind load increment factor λ is also defined to proportionally increase the wind load on the structure. Therefore, the wind loads acting on the structure are $\lambda \cdot \hat{p}$, and the critical value of λ can be obtained, denoted as λ_e , by nonlinear static stability analysis. Eq. (3) has shown that the static stability analyses for obtaining λ_e and f_S are both based on the proportional loading strategy of the same mean wind loads \bar{p} , so these two computing processes are actually the identical process, and we have

$$\lambda_e \cdot \varphi_D = f_S \quad (5)$$

Substituting Eq. (4) into Eq. (5) yields

$$\lambda_e = f_D \tag{6}$$

Consequently, the static stability design under the dynamic instability-aimed ESWLs can produce the real dynamic instability factor in the dynamic wind field. Thus, the equivalence of such ESWLs is proved.

2.3 Method for determining dynamic instability-aimed ESWLs

The computational procedure of the method for dynamic instability-aimed ESWLs for dynamic stability design can be divided into two steps.

The first step accomplished by wind engineering researchers is obtaining the dynamic instability-aimed ESWLs on the structure through the following procedures:

- (1) The unsteady aerodynamic forces on the structures in all the selected wind directions are obtained by wind tunnel tests.
- (2) The dynamic stability analysis of the structural system is conducted to acquire dynamic instability that originates from critical wind load incremental factor f_D in different wind directions and determine the most unfavorable wind direction.

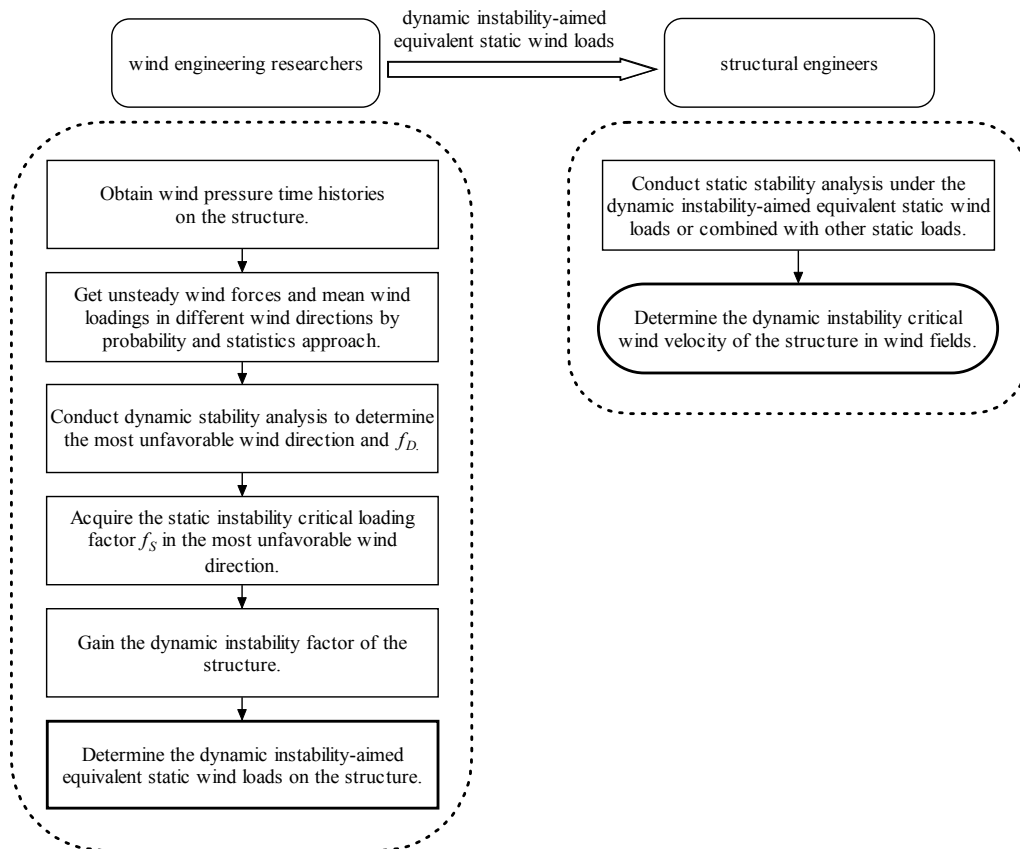


Fig. 1 Dynamic stability design of spatial structures in wind fields

The wind direction that has the smallest f_D is defined as the most unfavorable wind direction. The structural safety in the stability perspective in all wind directions can be ensured if it is guaranteed in the most unfavorable wind direction. Thus, only the acquisition of dynamic instability-aimed ESWLs and the dynamic stability design in such wind direction are necessary to be conducted.

(3) The static stability analysis of the structural system is carried out to obtain the critical wind load incremental factor f_S under mean wind load in such direction.

(4) After f_S and f_D are acquired, the corresponding dynamic instability factor φ_D can be computed by Eq. (4). The dynamic instability-aimed ESWLs on the structure can then be obtained using Eq. (3).

The second step carried out by structural engineers is conducting the static stability analysis of structures under the action of the dynamic instability-aimed ESWLs:

(5) The static stability analysis of the structural system under the dynamic instability-aimed ESWLs is conducted to obtain the dynamic instability caused by critical wind velocity. The wind resistance capacity of the structure can subsequently be evaluated.

The entire procedure of the dynamic stability design of spatial structures in wind fields is summarized in Fig. 1.

3. Applications

The method for determining dynamic instability-aimed ESWLs is applied in the dynamic stability design of a double-layer cylindrical reticulated shell located in a typhoon-prone area. First, the FEM model and free vibration analysis of the shell are introduced. Unsteady wind forces on the shell are then constructed on the basis of wind tunnel tests, and the dynamic stability analysis of the shell is carried out. The aeroelastic effects are not considered in the dynamic stability analysis. Actually, according to our research experience on the dynamic response analysis and wind-resistant design of more than 100 large span roof structures, the aeroelastic effects can be ignored for most large span roof structures. Especially, for the structural dynamic instability, the influence of aeroelastic effects could be smaller. The results of dynamic stability analysis are compared with those of static stability analysis under the ESWLs based on the equivalence of displacement and internal force. Finally, dynamic instability-aimed ESWLs on the shell are obtained, and the dynamic stability design of the shell is completed.

3.1 Free vibration analysis

Before studying the dynamic stability of the double-layer cylindrical reticulated shell under wind actions, the free vibration analysis of the shell should be conducted to understand its natural vibration characteristics. The FEM model of the shell is first introduced, and then the results of the free vibration analysis are discussed.

The double-layer cylindrical reticulated shell is a dry coal shed in a power plant, with a span of 103 m, longitudinal length of 140 m, and height of 40 m (Fig. 2). The shell is composed of crossing bars arranged as an orthogonal spatial grid. Thirteen types of bars with different areas are used in the shell (Table 1). The shell structure is discretized with truss elements, which simulate the dual-force bars of the shell. The Young's modulus of the bars is 206 GPa, and their density is

9400 kg/m³ which includes a 20% increment for considering the weight of joints. The linkage among the bars is modeled as hinged to allow for actual mechanical behavior, and the longitudinal base of the shell is modeled as rigid constraints to make the shell structure geometric invariant. The cladding material on the shell is simulated by the additional mass that is concentrated on the node.

The natural frequencies and corresponding modal shapes of the shell are obtained by free vibration analysis. The first 100 orders of natural frequency of the shell are highly intensive (Fig. 3), in which the first order and the 100th order of frequency are $f_1 = 1.38$ Hz and $f_{100} = 12.2$ Hz, respectively. The first order of modal shape of the shell is longitudinal deformation (Fig. 4(a)). No wind action along the longitudinal direction of the shell is observed; thus, the primary displacement of the shell under wind flows may not be similar to this modal shape. The second order of modal shape of the shell is transverse deformation (Fig. 4(b)); hence, the dominating displacement of the shell under perpendicular wind flows may be along the transverse direction. The third order of modal shape of the shell is torsional deformation (Fig. 4(c)), which causes both two ends of the shell to deform transversely along the opposite direction. Therefore, the dominating displacement of the shell under yawed wind flows may be similar to this deformation shape.

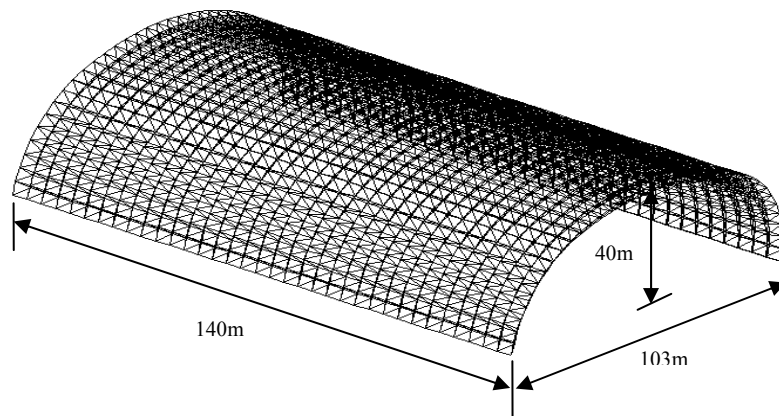


Fig. 2 3D-FEM model of the shell

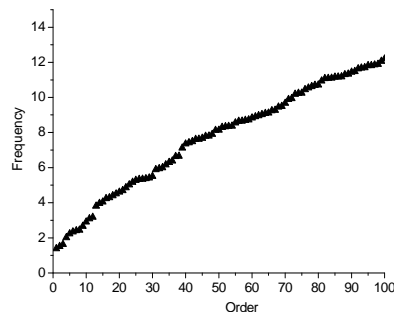


Fig. 3 First 100 orders of natural frequency of the shell

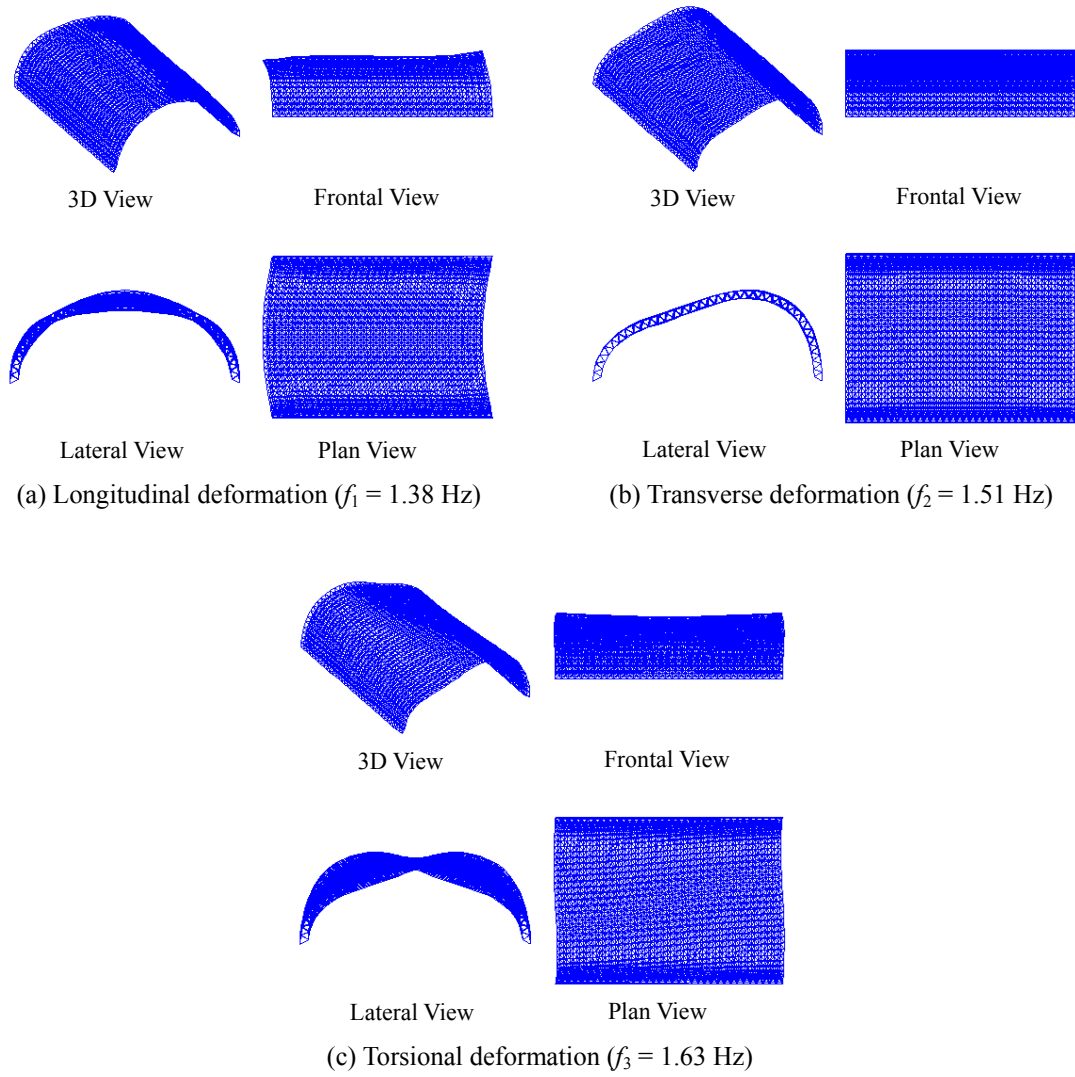
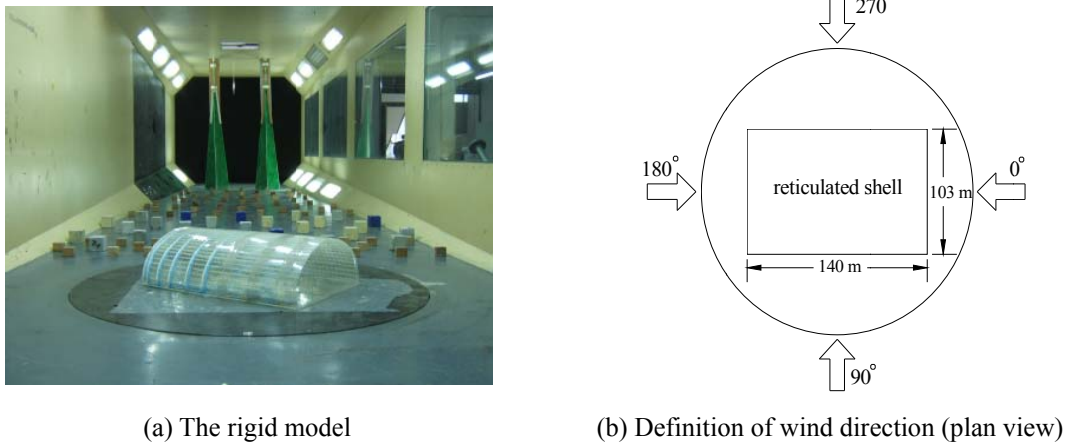


Fig. 4 First three orders of modal shape of the shell

Table 1 Area of bars in the shell

Type	1	2	3	4	5	6	7
Area/cm ²	8.52	10.68	13.82	17.09	28.84	37.95	53.41
Type	8	9	10	11	12	13	
Area/cm ²	57.81	78.04	90.16	100.04	115.11	141.37	



(a) The rigid model

(b) Definition of wind direction (plan view)

Fig. 5 Arrangements in wind tunnel tests

3.2 Wind tunnel tests

Wind loading on the structure is usually regarded as a stationary random process, and wind pressure time histories obtained from the wind tunnel tests can present long-term wind actions on the structure. In this section, the arrangements of wind tunnel tests and testing results are presented, and then the unsteady wind forces on the shell are constructed by the probability and statistics method.

The wind tunnel tests were carried out in TJ-2 atmospheric boundary layer wind tunnel (Tongji University, China), which has a working section 3 m wide, 2.5 m high, and 15 m long. A rigid model (Fig. 5(a)) with a geometric length scale of 1:150 was constructed to represent the shell. Both the outer and inner faces of the shell are exposed to wind flows. Thus, a couple of pressure taps were installed at a single measurement point on the model to simultaneously measure wind pressures on both faces; the net wind pressure at the measurement point is the difference of the pressures on both faces (Simiu and Scanlan 1996). Wind direction is defined as an angle β from the east along a clockwise direction (Fig. 5(b)). Seven types of wind tunnel tests with β varying from 90° to 180° with an incremental step of 15° were carried out in accordance with the symmetry of the shell.

Spires and roughness elements were set up to simulate the boundary layer wind flow of the suburban terrain type stipulated in the Load Code of China (Ministry of Housing and Urban-Rural Development of the People's Republic of China, 2001) as exposure B category. This terrain type specifies the mean wind velocity profile with a power law exponent of $\alpha = 0.16$. The measured turbulence intensity at the roof top is about 0.11, and the simulated power spectra of fluctuating wind agrees well with the Karman-type spectra.

In the wind tunnel tests, the wind pressures on the shell were measured simultaneously from all taps, and the data sampling frequency was 312.5 Hz with a sampling length of 6000 data. When processing the pressure data, the length of PVC pipes was set as an optimal parameter to optimize the measurement system (Zhou *et al.* 2011), except when directly modifying the measurement system. In the tests, the pressure measurements were carried out at a wind velocity of $U_{\text{ref}} = 12$ m/s at a reference height of $Z_{\text{ref}} = 100$ cm. The pressure coefficients of the measurement point i on the model are defined as

$$C_{pi} = \frac{p_i - p_\infty}{p_0 - p_\infty} \quad (7)$$

where p_i is the measured net pressure at measurement point i ; p_0 and p_∞ are the total and static pressures at the reference height, respectively.

The double-layer cylindrical reticulated shell is located in the most active typhoon-generating area in China, and the design wind velocity with a 50-year return period for the area is 55.2 m/s at a height of 150 m (35.8 m/s at 10 m) (Ministry of Housing and Urban-Rural Development of the People's Republic of China, 2001). Therefore, the wind velocity scale in the wind tunnel tests is 1/4.6, and the time scale is 1/32.6. The sampling frequency and record length T_{total} in the pressure measurements are equal to 9.58 Hz and 10.4 min at full scale, respectively. The period for evaluating the statistics of pressure fluctuations can be assumed to be 10 min, which is typically used as the average time in wind velocity measurements in China.

The pressure at measurement point i is analyzed as the mean and RMS pressure coefficients, $C_{p_{mean}}$ and $C_{p_{rms}}$, by the probability and statistics approach (Figs. 6-9). In Figs. 6-9, the straight line at the vertical center denotes the peak position of the cylindrical shell. The mean pressure coefficients are visibly distributed as stepped on the shell. Wind pressures are almost positive on the windward side and negative at the top area because wind flow separates at the top area. Wind pressures on the leeward side are also positive because wind flow reattaches in this area (Li and Melbourne 1995). The distribution of RMS pressure coefficients is different from that of mean pressure coefficients, and RMS coefficients are mostly distributed irregularly. Under yawed wind directions, wind pressures fluctuate more sharply and wind flow separation causes these pressures to fluctuate most sharply on the windward rim of the shell. Then, unsteady wind forces F_{0ij} of measurement point i at moment t_j at full scale can be constructed.

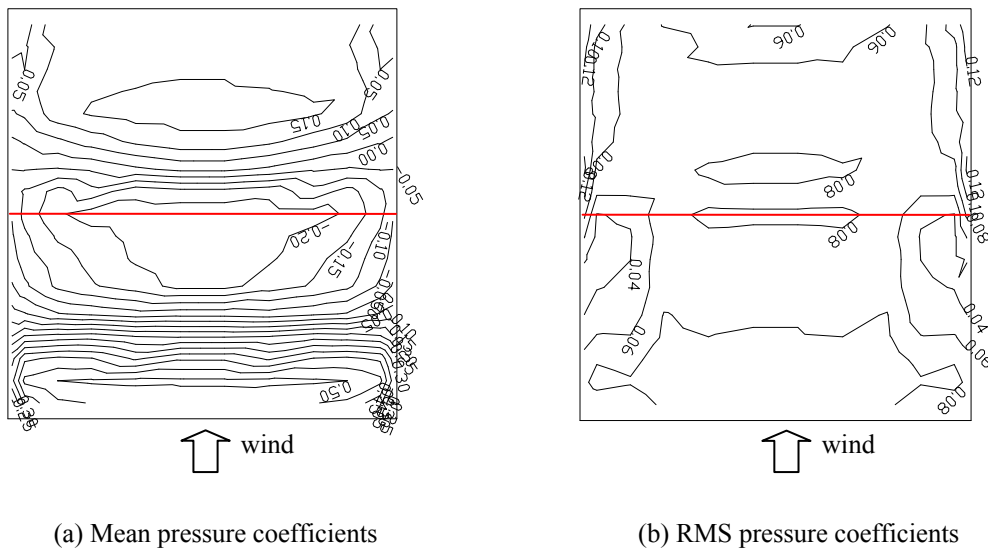
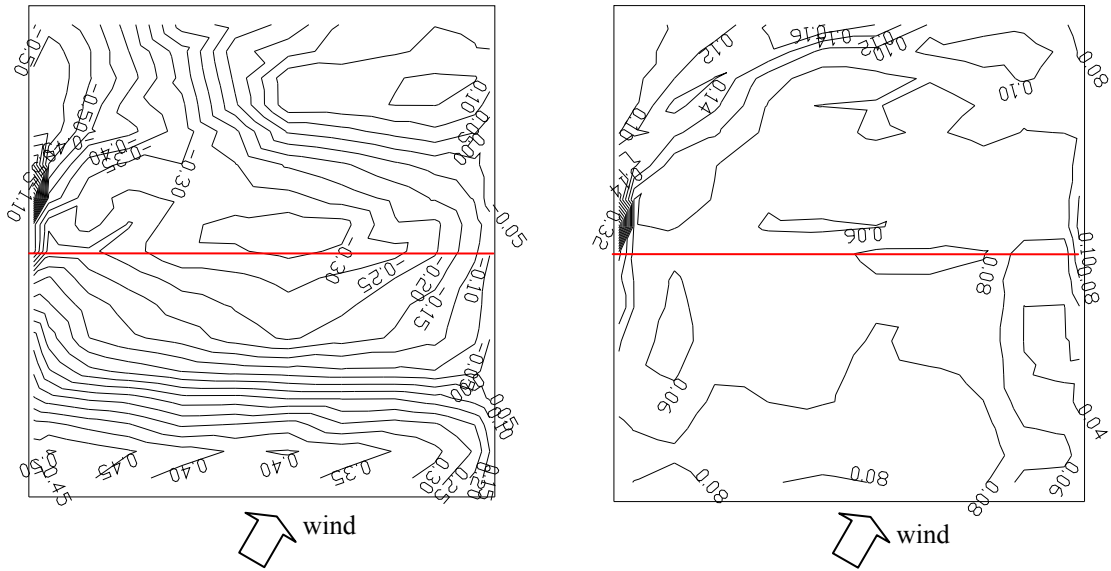


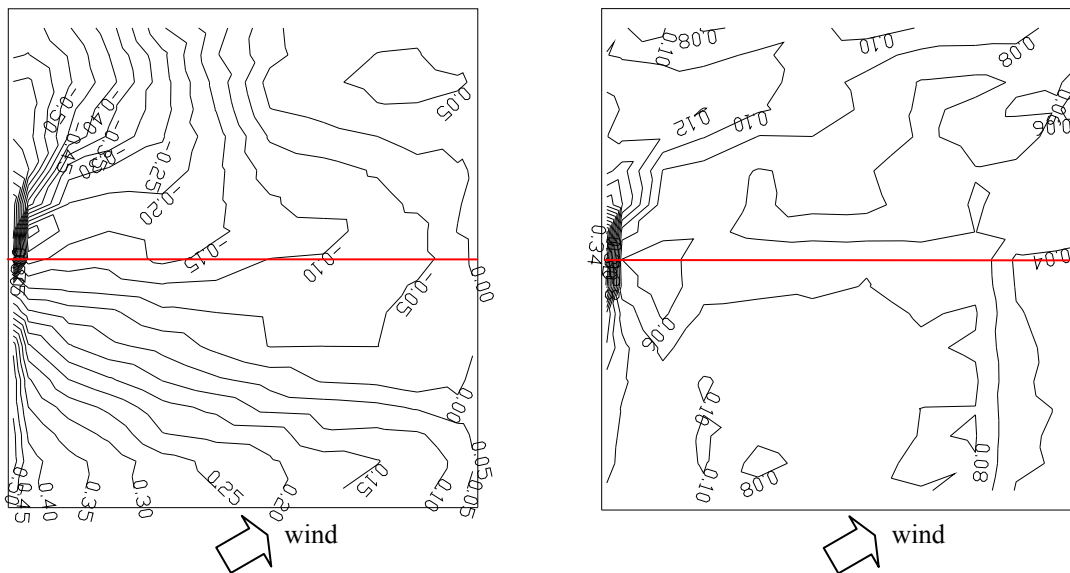
Fig. 6 Distribution of pressure coefficients on the shell in 90° (plan view)



(a) Mean pressure coefficients

(b) RMS pressure coefficients

Fig. 7 Distribution of pressure coefficients on the shell in 120°(plan view)



(a) Mean pressure coefficients

(b) RMS pressure coefficients

Fig. 8 Distribution of pressure coefficients on the shell in 150° (plan view)

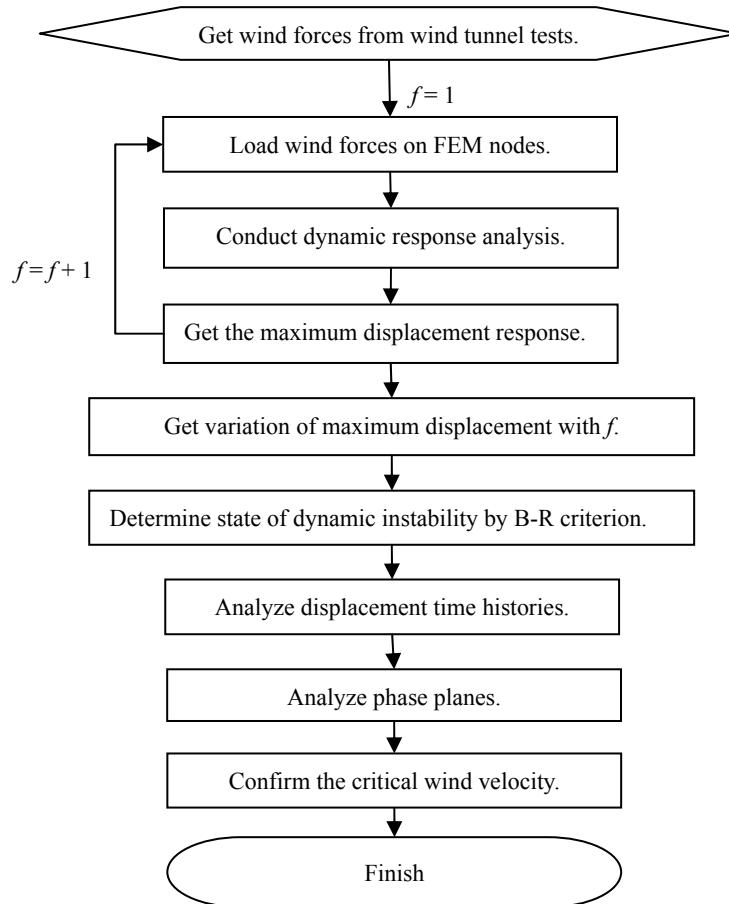


Fig. 10 Process of dynamic stability analysis under wind flows

According to the results of the dynamic response computation, the maximum displacement response w_{\max} of the shell generally increases in all wind directions with increasing wind velocity (Fig. 11). When f reaches a specific value, the displacement responses abruptly increase, so the shell becomes dynamically unstable according to the B–R criterion. The most obvious trend of instability occurs in the wind direction of 150° , and f_D is preliminarily selected as $1.0 \sim 2.0$. Hence, the most unfavorable wind direction is 150° , and the corresponding dynamic instability shape of the shell is shown in Fig. 12. The upwind region (the left half of the shell along the wind direction) of the shell deforms much more than does the downwind region. The windward area of this region moves downward, and the leeward area moves upward under positive and negative wind pressures, respectively (Fig. 8). Under the simultaneous actions of outward and inward wind forces on the two opposite sides of the upwind region, the shell is prone to deformation, which may be the primary reason for 150° being the most unfavorable direction.

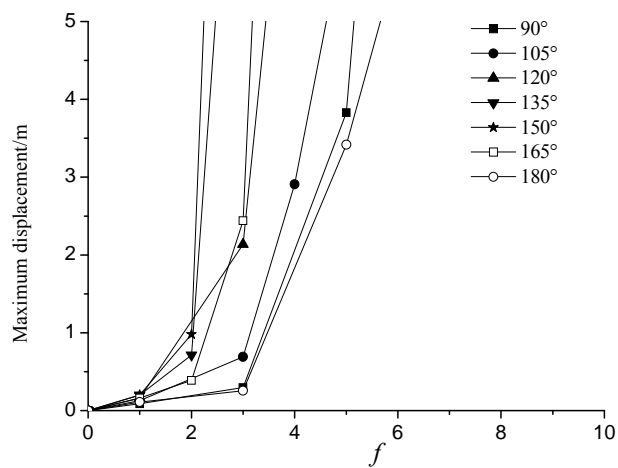
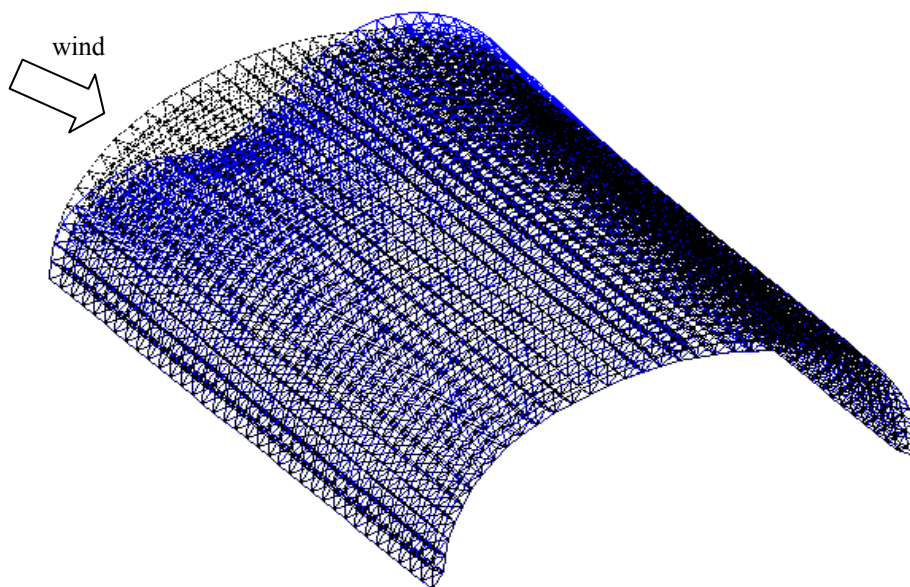
Fig. 11 Variation in the maximum displacement response with f 

Fig. 12 Dynamic instability shape of the shell (with undeformed shape)

The node that produces maximum displacement response w_{\max} is defined in this study as the characteristic node. The characteristic node produces the maximum displacement response of the shell; thus, its displacement time histories represent the response characteristics of the shell system to a certain extent. By investigating the displacement time histories of the characteristic nodes under different f (Fig. 13), the critical wind velocity-induced dynamic instability of the shell can be further determined. In Fig. 13, the straight line represents the displacement of the characteristic node under the gravity and mean wind load under the same f .

In the 150° wind direction, the characteristic node oscillates stably around the static equilibrium position during the entire wind duration under $f = 1.0$ (Fig. 13(a)). Thus, the trend of dynamic instability on the shell does not exist when f is less than 1.0.

However, when f reaches 1.5 and 2.0, the characteristic node moves past the static equilibrium position immediately after wind forces are loaded, and jumps at about $t = 40$, 70, and 450 s (Figs. 13(b) and 13(c)). Under $f = 2.0$, its dynamic equilibrium position shifts from 0.5 to 0.77 m away from the original configuration of the shell at $t = 70$ s. Therefore, the critical wind load-induced dynamic instability of the shell is conservatively chosen as $f_D = 1.0$.

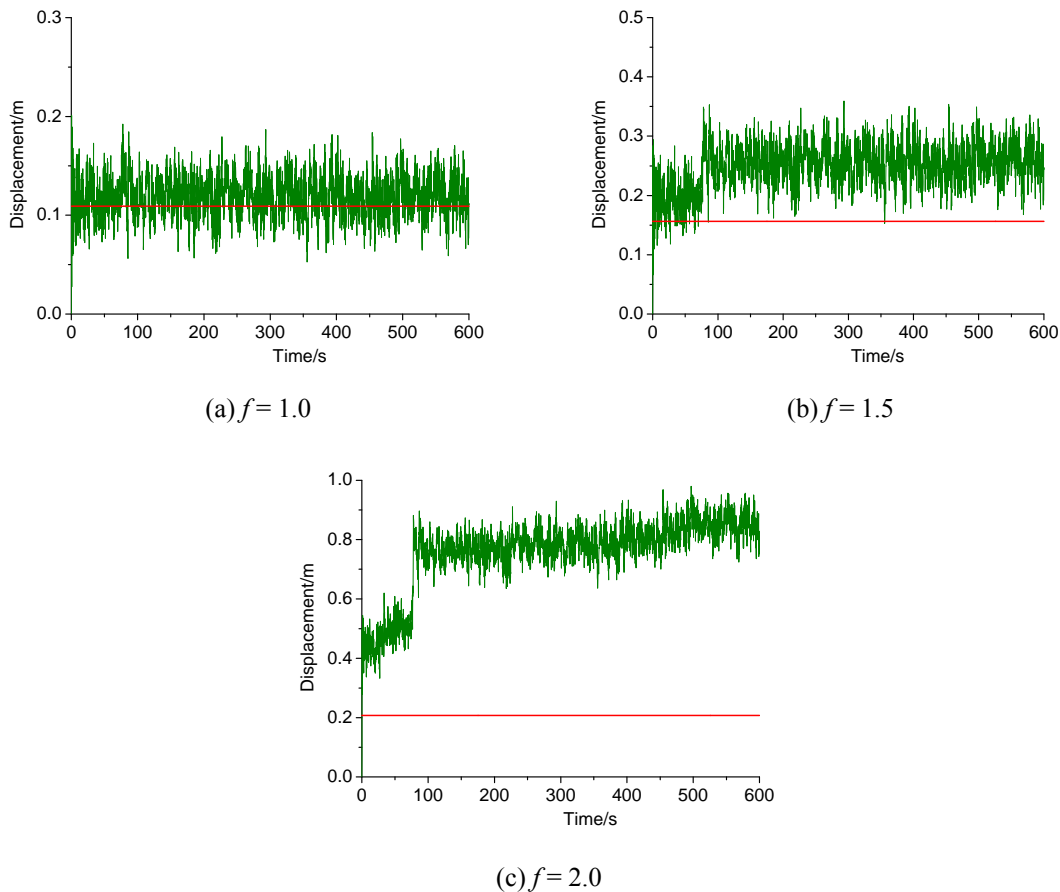


Fig. 13 Displacement time histories of the characteristic nodes in 150°

Meanwhile, according to the theory of the phase plane (Timpledon *et al.* 2010), the state point moves clockwise along the oval track on the phase plane when the structural system is dynamically stable. Therefore, if the state point goes off the oval track and turning points occur, the structural system becomes dynamically unstable.

Fig. 14 gives the displacement–velocity phase plane of the characteristic node under different f in 150° , which indicates that the state point visibly moves clockwise along the oval track on the phase plane when f is equal to 1.0. Thus, the shell is dynamically stable. However, when f reaches 2.0, obvious jumping on the phase plane is observed. The state point moves clockwise and counter-clockwise alternately, and turning points appear on the phase plane (Fig. 15); hence, the shell is dynamic unstable.

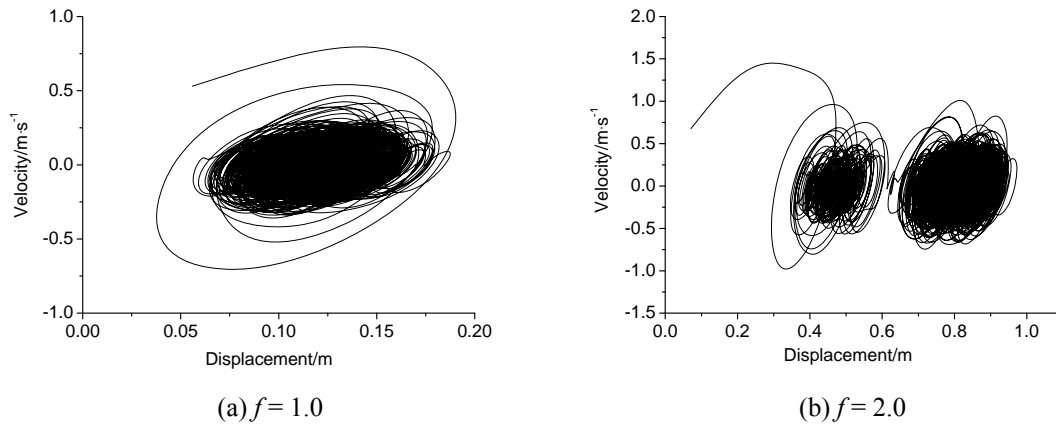


Fig. 14 Phase plane of the characteristic node in 150°

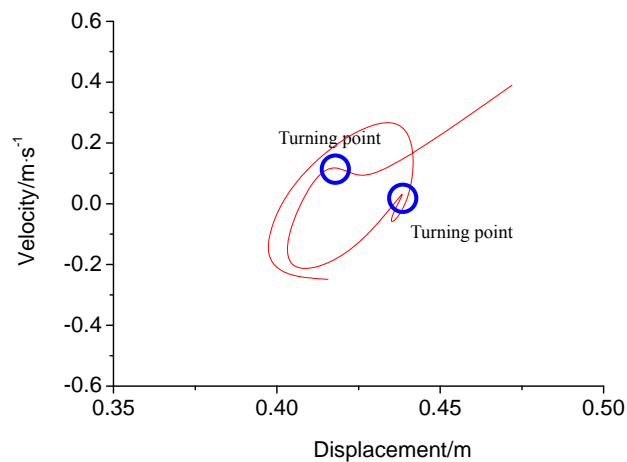


Fig. 15 Turning points on the phase plane at $f=2.0$ in 150°

Hence, the critical wind velocity-induced dynamic instability v_c of the shell can be

$$v_c = v_0 \times \sqrt{f_D} = 35.8 \times \sqrt{1.0} = 35.8 \text{ m/s} \quad (8)$$

where v_0 is the design wind velocity at a height of 10 m at full scale. The critical wind velocity-induced dynamic instability indicates that the shell may become dynamically unstable when the wind velocity of the area where the shell is located arrives at the design wind velocity of the shell. This is highly dangerous for spatial structures located in strong-wind environments.

3.4 Static stability design by ESWLs based on the equivalence of displacement and internal force

In general structural design considering wind loads, the ESWLs based on the equivalence of displacement or internal force of members, usually determined by the GLF method, is used to consider wind effects. Such ESWLs are used for static stability analysis to obtain a critical multiplier λ_{e-GLF} by the similar procedure for obtaining λ_e in section 2.2.

Mi (2007) carefully studied the ESWLs of the same double-layer cylindrical reticulated shell using the GLF method. The gust loading factors based on the equivalence of displacement or internal force was obtained vary between 1.29 and 1.74. The value of 1.74 is firstly used for stability design and the corresponding wind direction is 135° .

Thus, the ESWLs \hat{p}_{GLF} determined by the GLF method are

$$\hat{p}_{GLF} = 1.74 \bar{p}_{135} \quad (9)$$

where \bar{p}_{135} denotes the mean wind load in the wind direction of 135° .

According to the variation in maximum displacement response with λ (Fig. 16), λ_{e-GLF} is determined as 2.0. That is, if the ESWLs determined by the GLF method are used for the stability analysis, the shell would become unstable only when wind pressures are 2.0 times the design wind pressures. If the gust loading factor of 1.29 is used for computation, λ_{e-GLF} would be larger.

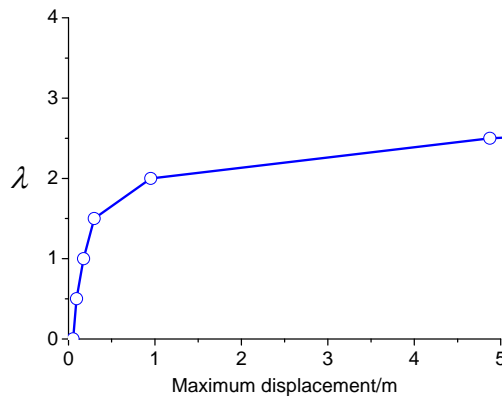


Fig. 16 Variation in the maximum displacement with λ under $\lambda \cdot \hat{p}_{GLF}$

However, according to the above-mentioned results of the dynamic stability analysis, the shell may become dynamically unstable when the wind loads is only 1.0 times the design wind loads. Therefore, the stability design of spatial structures by the ESWLs based on the equivalence of the displacement or internal force may lead to unreliable conclusions.

3.5 Dynamic stability design

The dynamic instability-aimed ESWLs on the double-layer cylindrical reticulated shell are obtained and then applied in the stability design of the shell.

3.5.1 Dynamic instability-aimed ESWLs

According to the results of the dynamic stability analysis, 150° is the most unfavorable direction of the dynamic stability of the shell in wind fields. Therefore, only the dynamic instability-aimed ESWLs in this wind direction are necessary.

According to the results of the static stability analysis under mean wind loads of 150° (Fig. 17), static instability critical wind load incremental factor f_S is equal to 3.5. Simultaneously, according to the above-mentioned dynamic stability analysis, the dynamic instability critical wind load incremental factor f_D at 150° is equal to 1.0. Therefore, according to Eq. (4), the dynamic instability factor φ_D is equal to 3.5.

According to Eq. (3), the dynamic instability-aimed ESWLs are

$$\hat{p}(x, y, z) = 3.5 \cdot \bar{p}(x, y, z) \quad (10)$$

where $\bar{p}(x, y, z)$ is the mean wind loads at 150° .

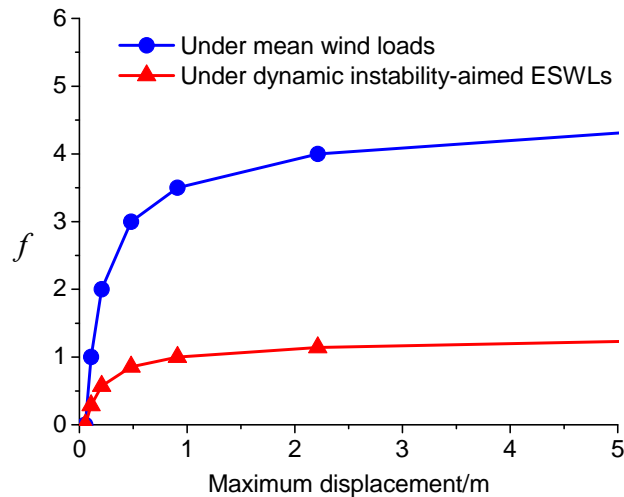


Fig. 17 Variation in the maximum displacement with f

3.5.2 Static stability analysis under dynamic instability-aimed ESWLs

According to the variation in the maximum displacement with loading parameter λ (Fig. 17), λ_e is equal to 1.0 by the method in Section 2.2. Therefore, the critical load parameter λ_e obtained here is identical to the dynamic instability critical factor f_D obtained from the dynamic stability analysis, which verifies Eq. (6). This clearly indicates that the actual dynamic instability in wind fields can be obtained by carrying out static stability design based on the dynamic instability-aimed ESWLs. Consequently, with the help of dynamic instability-aimed ESWLs, the accurate dynamic stability design of spatial structures in wind flows can be achieved by simpler static stability analysis.

Meanwhile, the results of dynamic stability design show that dynamic instability may occur in the double-layer cylindrical reticulated shell when the wind velocity is equal to the design wind velocity. However, the stability analysis under the ESWLs obtained by the GLF method indicates that structural instability may occur only if the wind velocity is more than $\sqrt{2.0}$ times the design wind velocity. Hence, dynamic stability design based on the dynamic instability-aimed ESWLs is accurate and much more conservative for structures.

4. Conclusions

The concept of dynamic instability-aimed ESWLs and its corresponding method have been proposed in this paper. The dynamic stability of spatial structures under unsteady wind forces can be studied by the experimental–numerical method, in which the state of dynamic instability can be determined by the B–R criterion combined with observations of the dynamic equilibrium position and phase plane of the characteristic node. The dynamic instability-aimed ESWLs can be obtained through the dynamic instability factor. Finally, the actual dynamic instability that stems from the critical wind velocity of spatial structures can be obtained by static stability analysis.

The dynamic instability factor is the core concept in the method for determining dynamic instability-aimed ESWLs. The factor denotes the extent of decrease in dynamic instability critical wind loads under unsteady winds compared with static instability critical wind loads under mean winds. The larger this factor is, the higher the influence of the dynamic effects of wind loads on wind-induced structural stability, and the more strongly the structure is subjected to dynamic instability. The range of the dynamic instability factor represents different characteristics of structural dynamic stability. When the factor is equal to 1.0, the dynamic wind effects have no influence on the stability of the structure, and the dynamic wind loads can be treated as static wind loads in stability analysis. This case holds true for rigid structures. When the factor is less than 1.0, the critical wind load of dynamic instability is higher than that of static instability, so the dynamic load effects make the structure more stable in wind fields, a phenomenon that seldom happens. When the dynamic instability factor is larger than 1.0, the critical wind load of dynamic instability is lower than that of static instability. Consequently, the dynamic wind effects will impose a negative influence on structural stability, and such structures become prone to dynamic instability. This is the most common case in spatial structures.

For the double-layer cylindrical reticulated shell, the dynamic instability-aimed equivalent static wind load of the shell is about two times the ESWLs based on the equivalence of displacements or internal forces. Therefore, the shell may become unstable under the dynamic instability-aimed ESWLs even when it is stable under the ESWLs determined on the basis of the equivalence of response or internal force. The yawed wind direction is the most unfavorable wind direction for the dynamic instability of the shell, in which the shell becomes dynamically unstable

below its design wind velocity. When the shell is dynamically unstable, the dynamic equilibrium position of the characteristic node may jump several times, the state point moves clockwise and counter-clockwise alternately on the displacement–velocity phase plane of the characteristic node, and the shell eventually collapses to the ground.

Acknowledgments

This project is jointly supported by the National Natural Science Foundation (50621062; 51208126) and State Key Laboratory Foundation (SLDRCE08-A-03).

References

- Bartoli, G. and Ricciardelli, F. (2010), “Characterisation of pressure fluctuations on the leeward and side faces of rectangular buildings and accuracy of the quasi-steady loads”, *J. Wind Eng. Ind. Aerod.*, **98**(10-11), 512-519.
- Budiansky, B. and Roth, R.S. (1962), *Axisymmetric dynamic buckling of clamped shallow spherical shells*, NASA TND-510, Washington D.C., 597-606.
- Cao, Y., Wang, P. and Jin, X. (2010), “Dynamic analysis of flexible container under wind actions by ALE finite-element method”, *J. Wind Eng. Ind. Aerod.*, **98**(12), 881-887.
- Chen, B., Yang, Q. and Wu, Y. (2012), “Wind-induced response and equivalent static wind loads of long span roofs”, *Adv. Struct. Eng.*, **15**(7), 1099-1114.
- Davenport, A.G. (1961), “The application of statistical concepts to the wind loading of structures”, *Proceedings of the Institution of Civil Engineers*, **19**(4), 449-472.
- Davenport, A.G. (1967), “Gust Loading Factor”, *J. Struct. Div.*, **93**(ST3), 11-34.
- Davenport, A.G. (1995), “How can we simplify and generalize wind loads”, *J. Wind Eng. Ind. Aerod.*, **54**, 657-669.
- Duthinh, D., Main, J.A., Wright, A.P. and Simiu E. (2008), “Low-rise steel structures under directional winds: Mean recurrence interval of failure”, *J. Struct. Eng.-ASCE*, **134**(8), 1383-1388.
- Fu, J., Xie, Z. and Li, Q. (2008), “Equivalent static wind loads on long-span roof structures”. *J. Struct. Eng.-ASCE*, **134**(7), 1115-1128.
- He, Y. (2002), “Aerodynamic stability analysis of space structures”, *J. Shanghai Jiaotong Univ.*, **36**(11), 1616-1620 (in Chinese).
- Hsu, C. (1967), “The effect of various parameters on the dynamic stability of a shallow arch”, *J. Appl. Mech. - T ASME*, **34**(6), 349-358.
- Huang, Y. and Gu, M. (2011), “Dynamic instability of spatial structures under wind loads”, *J. Vib. Shock*, **30**(2), 41-46 (in Chinese).
- Ishikawa, K. and Kato, S. (1993), “Earthquake resistant capacity of double layer latticed dome due to vertical motions”, *J. Struct. Constr. Eng.*, **447**(5), 79-88.
- Kasperski, M. (1992), “Extreme wind load distributions for linear and nonlinear design”, *Eng. Struct.*, **14**(1), 27-34.
- Katsumura, A., Tamura, Y. and Nakamura O. (2007), “Universal wind load distribution simultaneously reproducing largest load effects in all subject members on large-span cantilevered roof”, *J. Wind Eng. Ind. Aerod.*, **95**(9-11), 1145-1165.
- Ke, S., Wang, T., Ge, Y. and Tamura, Y. (2014), “Wind-induced responses and equivalent static wind loads of tower-blade coupled large wind turbine system”, *Struct. Eng. Mech.*, **52**(3), 485-505.
- Li, Q. and Melbourne, W.H. (1995), “An experimental investigation of the effects of free-stream turbulence on streamwise surface pressures in separated and reattaching flows”, *J. Wind Eng. Ind. Aerod.*, **54-55**,

- 313-323.
- Li, Y. and Tamura, Y. (2005), "Nonlinear dynamic analysis for large-span single-layer reticulated shells subjected to wind loading", *Wind Struct.*, **8**(1), 35-48.
- Liang S., Zou L., Wang D. and Huang G. (2014), "Analysis of three dimensional equivalent static wind loads of symmetric high-rise buildings based on wind tunnel tests", *Wind Struct.*, **19**(5), 565-583.
- Mi, F. (2007), "Research on wind-induced responses and interference effects on dry coal shed", Master Dissertation, Tongji University, Shanghai, China (in Chinese).
- Ministry of Housing and Urban-Rural Development of the People's Republic of China (2001), *GB50009-2001*, Load code for the design of building structures, Beijing (in Chinese).
- Ministry of Housing and Urban-Rural Development of the People's Republic of China (2003), *GB50017-2003*, Code for design of steel structures, Beijing (in Chinese).
- Miyake, A., Yoshimura, T. and Makino, M. (1992), "Aerodynamic instability of suspended roof models", *J. Wind Eng. Ind. Aerod.*, **42**(1-3), 1471-1482.
- Nakamura, O., Tamura, Y., Miyashita, K. and Itoh M. (1994), "A case study of wind pressure and wind-induced vibration of a large span open-type roof", *J. Wind Eng. Ind. Aerod.*, **52**, 237-248.
- Shanmugasundaram, J., Arunachalam, S., Gomathinayagam, S., Lakshmanan, N. and Harikrishna, P. (2000), "Cyclone damage to buildings and structures-a case study", *J. Wind Eng. Ind. Aerod.*, **84**(3), 369-380.
- Simitses, G. (1990), *Dynamic Stability of Suddenly Loaded Structures*, Springer-Verlag, New York, NY, USA.
- Simiu, E. and Scanlan, R.H. (1996), *Wind effects on structures: fundamentals and applications to design*, John Wiley&Sons, Inc., New York, NY, USA.
- Sofiyev, A.H. (2004), "The stability of functionally graded truncated conical shells subjected to aperiodic impulsive loading", *Int. J. of Solids Struct.*, **41**(13), 3411-3424.
- Song, B. and Jones, N. (1983), "Dynamic buckling of elastic-plastic complete spherical shells under step loading", *Int. J. Impact Eng.*, **1**(1), 51-71.
- Timpledon, L., Marseken, M. and Surhone, S. (2010), *Phase plane: Differential equation, Lotka-Volterra equation, eigenvectors, eigenvalues, saddle point, node, sines*, Betascript Publishing, Beau Bassin, Mauritius.
- Toi, Y. and Isobe, D. (1996), "Finite element analysis of quasi-static and dynamic collapse behavior of framed structure by the adaptively case study of wind pressure and wind-induced vibration shifted integration technique", *Comput. Struct.*, **58**(5), 947-955.
- Yang, Q. and Liu, R. (2005), "On aerodynamic stability of membrane structures", *Int. J. Space Struct.*, **20**(3), 181-188.
- Zhou, X., Huang, P., Gu, M. and Mi, F. (2011), "Wind loads and responses of two neighboring dry coal sheds", *Adv. Struct. Eng.*, **14**(2), 207-221.
- Zhou, X., Gu, M. and Li, G. (2012), "Grouping response method for equivalent static wind loads based on a modified LRC method", *Earthq. Eng. Eng. Vib.*, **11**(1), 107-119.
- Zhou, Y., Gu, M. and Xiang, H. (1999), "Along-wind static equivalent wind loads and responses of tall buildings. Part I: Unfavorable distributions of static equivalent wind loads", *J. Wind Eng. Ind. Aerod.*, **79**(1-2), 135-150